

AdipoRon enhances healthspan in middle-aged obese mice: striking alleviation of myosteatosi s and muscle degenerative markers

Camille M. Selvais^{1*} , María A. Davis-López de Carrizosa^{1,2}, Maxime Nachit³, Romain Versele¹, Nicolas Dubuisson¹, Laurence Noel¹, Justine Gillard³, Isabelle A. Leclercq³, Sonia M. Brichard¹ & Michel Abou-Samra¹ 

¹Endocrinology, Diabetes and Nutrition Unit, Institute of Experimental and Clinical Research, UCLouvain, Brussels, Belgium; ²Department of Physiology, Faculty of Biology, University of Seville, Seville, Spain; ³Hepato-Gastroenterology Unit, Institute of Experimental and Clinical Research, UCLouvain, Brussels, Belgium

Abstract

Background Obesity among older adults has increased tremendously. Obesity accelerates ageing and predisposes to age-related conditions and diseases, such as loss of endurance capacity, insulin resistance and features of the metabolic syndrome. Namely, ectopic lipids play a key role in the development of nonalcoholic fatty liver disease (NAFLD) and myosteatosi s, two severe burdens of ageing and metabolic diseases. Adiponectin (ApN) is a hormone, mainly secreted by adipocytes, which exerts insulin-sensitizing and fat-burning properties in several tissues including the liver and the muscle. Its overexpression also increases lifespan in mice. In this study, we investigated whether an ApN receptor agonist, AdipoRon (AR), could slow muscle dysfunction, myosteatosi s and degenerative muscle markers in middle-aged obese mice. The effects on myosteatosi s were compared with those on NAFLD.

Methods Three groups of mice were studied up to 62 weeks of age: One group received normal diet (ND), another, high-fat diet (HFD); and the last, HFD combined with AR given orally for almost 1 year. An additional group of young mice under an ND was used. Treadmill tests and micro-computed tomography (CT) were carried out in vivo. Histological, biochemical and molecular analyses were performed on tissues ex vivo. Bodipy staining was used to assess intramyocellular lipid (IMCL) and lipid droplet morphology.

Results AR did not markedly alter diet-induced obesity. Yet, this treatment rescued exercise endurance in obese mice (up to 2.4-fold, $P < 0.05$), an event that preceded the improvement of insulin sensitivity. Dorsal muscles and liver densities, measured by CT, were reduced in obese mice (−42% and −109%, respectively, $P < 0.0001$), suggesting fatty infiltration. This reduction tended to be attenuated by AR. Accordingly, AR significantly mitigated steatosi s and cellular ballooning at liver histology, thereby decreasing the NAFLD activity score (−30%, $P < 0.05$). AR also strikingly reversed IMCL accumulation either due to ageing in oxidative fibres (types 1/2a, soleus) or to HFD in glycolytic ones (types 2x/2b, extensor digitorum longus) (−50% to −85%, $P < 0.05$ or less). Size of subsarcolemmal lipid droplets, known to be associated with adverse metabolic outcomes, was reduced as well. Alleviation of myosteatosi s resulted from improved mitochondrial function and lipid oxidation. Meanwhile, AR halved aged-related accumulation of dysfunctional proteins identified as tubular aggregates and cylindrical spirals by electron microscopy ($P < 0.05$).

Conclusions Long-term AdipoRon treatment promotes ‘healthy ageing’ in obese middle-aged mice by enhancing endurance and protecting skeletal muscle and liver against the adverse metabolic and degenerative effects of ageing and caloric excess.

Keywords adiponectin; myosteatosi s; intramyocellular lipids; ageing; nonalcoholic fatty liver disease; endurance

Received: 13 October 2022; Accepted: 16 November 2022

*Correspondence to: Camille Selvais, Endocrinology, Diabetes and Nutrition Unit, Institute of Experimental and Clinical Research, UCLouvain, Brussels, Belgium.
Email: camille.selvais@uclouvain.be

Introduction

As society ages, the incidence of physical limitations is dramatically increasing. An important cause of physical limitations is the age-related loss of skeletal muscle mass, referred to as sarcopenia. Muscle function is impaired as well, and the endurance capacity declines.¹ Beyond physical performance, muscles also play a crucial role in insulin sensitivity and fuel homeostasis. Muscle disturbances may thus contribute to insulin resistance and metabolic syndrome.¹

Obesity among older adults aged 65 and over has increased noticeably over the last decades on all continents, and its prevalence is reaching 35% in the United States where it is expected to at least double by 2050.² Obesity accelerates ageing and predisposes an individual to age-related conditions and diseases. Thus, obesity and ageing go hand in hand with loss of muscle mass, function and endurance capacity, insulin resistance, and features of the metabolic syndrome.³ Two additional burdens associated with this syndrome involve ectopic lipid deposition in the liver and the skeletal muscle, namely, nonalcoholic fatty liver disease (NAFLD)/steatohepatitis (NASH) and myosteatorosis, whose rising prevalence tends to parallel that of obesity and ageing.^{4,5}

Adiponectin (ApN) is a hormone, mainly secreted by the adipose tissue, which is known to be tightly linked to the metabolic syndrome. ApN exerts insulin-sensitizing, fat-burning and anti-inflammatory actions, thereby effectively counteracting several facets of this syndrome. Liver and muscle are two of its main target tissues. The ApN receptor, AdipoR2 is predominantly expressed in the liver, whereas AdipoR1 is predominantly expressed in the skeletal muscle. In the liver, ApN stimulates fatty-acid oxidation and reduces glucose production.⁶ In skeletal muscle, we have shown that ApN does also exert powerful protective effects in mdx mice, a model with a severe muscle disease (Duchenne muscular dystrophy). Thus, ApN reduces muscle inflammation and oxidative stress and enhances the myogenic program, thereby decreasing muscle damage while increasing force/endurance.^{6,7} Importantly, overexpression of ApN in transgenic mice prolongs life span⁸ whereas complete deficiency of ApN in knockout mice shortens it.⁹

ApN has a complex three-dimensional structure and must be injected to produce its effects.⁶ The development of novel molecules that mimic the beneficial effects of ApN is therefore relevant. AdipoRon is an orally active synthetic agonist of ApN receptors, which, based on data in animal models, has been proposed for the treatment of type 2 diabetes and other obesity-related disorders.^{10–12} Relevant for translational applications, AdipoRon remains efficient in AdipoR1-humanized mice.¹³ We have recently shown that, like ApN, AdipoRon protects the skeletal muscle of mdx mice.¹⁴ However, its potential beneficial properties on ageing muscle have been scarcely addressed.¹⁵ It is also un-

known whether this molecule does effectively prolong life span in normal (wild-type) mice. An effect on longevity has been observed in a mouse model with a severe form of genetic diabetes; hence, the marked alleviation of diabetes provoked by AdipoRon was, in this case, a major confounding factor.¹⁰

The overall aim of this work was to explore whether AdipoRon could promote healthy ageing in middle-aged obese mice on a normal genetic background. Mice were rendered obese by chronic excess of caloric intake in order to mimic our western-life style habits and the high prevalence of obesity in the elderly. Some of these mice were concomitantly treated with AdipoRon for approximately 1 year. Herein, we investigated whether an ApN receptor agonist, AdipoRon, could slow down muscle dysfunction, myosteatorosis and degenerative muscle markers in middle-aged obese mice. The effects on myosteatorosis were compared with those on NAFLD.

Methods

Experimental design and animals

Male C57BL/6J mice were divided into three groups and studied up to 62 weeks of age. They are referred to as old (O) mice (*Figure 1A*). Two of these groups received a high-fat diet (HFD): mice in one HFD group were orally treated with AdipoRon (AR) for approximately 1 year (30 mg/kg/day scaled up to 50 mg/kg/day; O-HFD + AR), while mice in the other group were left untreated (O-HFD). HFD groups were compared with O mice kept on a normal diet (O-ND). An additional group of young (12-week-old) mice under a normal diet (Y-ND) was also studied. Mice were subjected to treadmill exhaustion tests at 32 and 56 weeks of age and to micro-computed tomography (CT) at 59 weeks. Histological, biochemical and molecular analyses were performed on tissues *ex vivo*. Mice were purchased from Janvier Labs, Genest, France, and AdipoRon from Bio-Techne, Minnesota, USA. Please see the *Supporting Information S1* for detailed experimental procedures.

Results

Long-term administration of AdipoRon protects against impaired glycaemia, dyslipidaemia and improves endurance

The body weight of O-HFD mice steadily increased and was twice that of O-ND animals at the end of study (*Figure 1B*). In line with others,¹⁰ AdipoRon did not markedly alter obesity and only stabilized the body weight at the end of

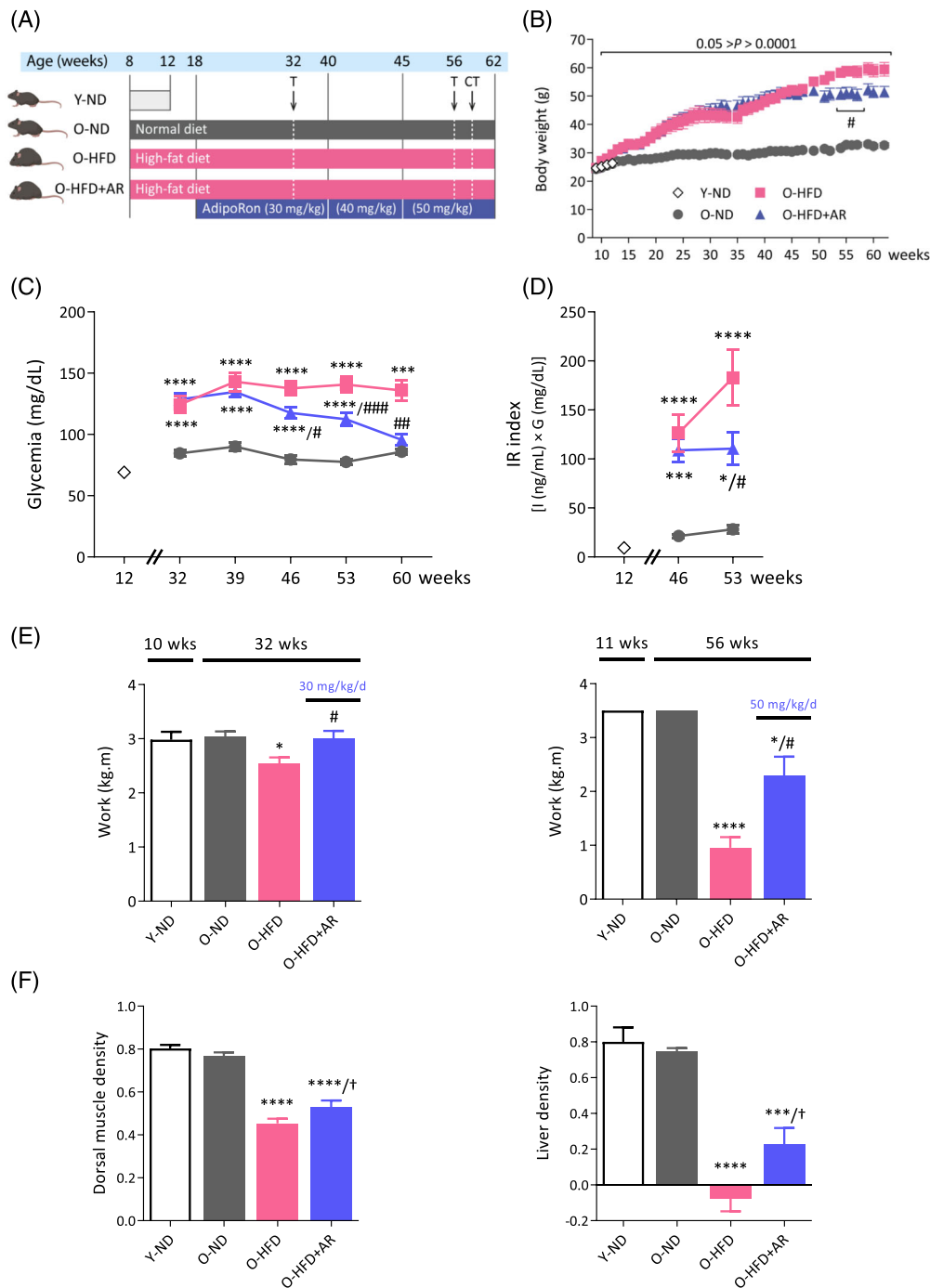


Figure 1 Chronic administration of AdipoRon improves insulin sensitivity, endurance and enhances computed tomography (CT) scan muscle and liver densities in middle-aged obese mice. (A) Experimental protocol. Four groups of mice were studied. Three groups were studied up to 62 weeks of age and are referred to as old (O) mice. Two of these groups received a high-fat diet (HFD) from 8 weeks. One HFD group was orally treated with AdipoRon (AR), starting from 18 weeks (30 mg/kg/day scaled up to 50 mg/kg/day; O-HFD + AR), while the other one was left untreated (O-HFD). Both groups were compared with O mice kept on a normal diet (O-ND). An additional group of young (12-week-old) mice under a normal diet (Y-ND) was also used for comparison. At the indicated times, mice were submitted to treadmill exhaustion test (T) or micro-CT. (B–D) Evolution of body weight, glycaemia and insulin resistance index during the study. (E) Mice were submitted to an uphill treadmill exhaustion test at different ages, with each time a protocol adapted to mice conditions. Endurance capacity was expressed as work to consider the differences in body weight (kg) over the distance covered (m). (F) Micro-CT evaluation of dorsal muscle and liver density, a decrease in density reflecting fatty infiltration. Data are means \pm SEM for 6 Y-ND, and 9–12 mice in the other three groups. Statistical analysis was performed using a mixed-effects analysis (B) or one-way ANOVA followed by Tukey's test to compare the three groups of O mice (C–F). Comparisons between Y-ND and O-ND were carried out using unpaired two-tailed *t*-test. **P* < 0.05, ****P* < 0.001, *****P* < 0.0001 versus O-ND mice. †*P* \leq 0.07, #*P* < 0.05, ###*P* < 0.01, ####*P* < 0.001 versus O-HFD mice.

the protocol. Likewise, daily energy intake, which was approximately 60% higher under HFD, was not modified by AdipoRon (Figure S1). Yet AdipoRon, when administered at the highest dose (50 mg/kg/day), progressively decreased fasting blood glucose levels, which were moderately elevated in HFD-fed mice, to reach O-ND values (Figure 1C). The insulin resistance index was attenuated as well (Figure 1D). Moreover, AdipoRon decreased plasma cholesterol levels induced by HFD, possibly through increased efflux, without modifying other circulating lipids (Table S1). Plasma ApN levels were decreased in old mice compared with young ones (O-ND vs. Y-ND), and this decrease was further amplified in obese mice when data were normalized by white fat mass (i.e., expressed per 'secretion unit'¹⁶; Table S1).

We next evaluated the effect of AdipoRon on muscle function by using an uphill treadmill exhaustion test. This test was performed twice, with each time a protocol adapted to age and obesity of the mice (Figure 1E, see Supporting information). At 32 weeks, exercise endurance capacity, expressed as work, was reduced in O-HFD mice compared with O-ND ones and was corrected by AdipoRon. At 56 weeks, work of O-HFD was drastically reduced (73% vs. O-ND), while it was partially rescued by AdipoRon. Thus, AdipoRon was able to partially or totally rescue exercise endurance of middle-aged obese mice. This already occurs at the low dose of AdipoRon (30 mg/kg/day), which did affect neither glucose homeostasis nor the body weight (compare Figure 1E left panel vs. Figure 1B,C).

Effects of AdipoRon on body composition, and liver and muscle density

We measured in vivo the body composition of mice as well as liver and muscle density by micro-CT. Whole body fat mass, which was markedly increased in O-HFD mice, was reduced by 20% under AdipoRon treatment (Figure S1B), in line with the decreased subcutaneous fat measured ex vivo (Table S1). However, AdipoRon did not significantly alter total lean mass (Figure S1C), in agreement with the unchanged dorsal muscle area, an index of muscle mass¹⁷ (Figure S1D) and the unchanged weight of several muscles sampled ex vivo (Table S1). Dorsal muscle density was decreased in HFD mice, suggesting fatty infiltration (Figure 1F, left). However, this decrease tended to be less pronounced under AdipoRon treatment, a result confirmed *a posteriori* by lipid dosage of dorsal muscle (Figure S1E). Likewise, liver density was reduced in both groups of HFD-mice, but this reduction also tended to be attenuated by AdipoRon (Figure 1F, right). These data suggest therefore that AdipoRon treatment lessens hepatic steatosis and myosteatosis induced by HFD.

AdipoRon reduces the severity of NAFLD

To further investigate the effects of AdipoRon on the liver, several parameters including steatosis, hepatocellular ballooning and inflammation were quantified on histological sections using the NAFLD activity score (NAS score) (Figure 2A,B). O-ND mice had almost normal liver histology (NAS = 0.4). O-HFD mice were diagnosed with nonalcoholic steatohepatitis (NASH) (i.e., $NAS \geq 3$ with at least 1 point in each sub-score) as they exhibited steatosis (>2), inflammation (>2) and ballooning (>1). By contrast, O-HFD + AR mice did not reach NASH stage: They had lower scores of steatosis (<2), inflammation (<2) and ballooning (<1). Strikingly, only 3 out of 10 O-HFD + AR mice presented ballooning versus 7 out of 8 in untreated HFD ones. The protective effect of AdipoRon on steatosis was corroborated by liver lipid dosage and liver weight (Figure 2C; Table S1). These data indicate that AdipoRon partially protected against liver fatty infiltration and mitigated the severity of NAFLD in diet-induced obese mice.

AdipoRon drastically blunts diet- or age-induced accumulation of Intramyocellular lipids

We next examined the effects of AdipoRon on myosteatosis and more specifically on the excessive accumulation of intramyocellular lipids (IMCLs) that leads to insulin resistance in obesity and type 2 diabetes.^{18,19} With this accumulation being fibre type-dependent, we quantified IMCL content and analysed lipid droplet (LD) morphology in the soleus, a slow-twitch oxidative muscle, and in the *extensor digitorum longus* (EDL), a fast-twitch glycolytic one. We performed fibre typing and LD staining on serial muscle cryosections.

The total number of fibres in each muscle was similar between the four groups of mice (data not shown). Fibre typing was carried out by immunofluorescence staining of different MyHCs isoforms (Figure 3A). As expected, the soleus contained a large proportion of slow-oxidative type 1 (blue, ~38%) and 2a fibres (green, ~50%), whereas the EDL was mainly composed of fast-glycolytic type 2b (black, ~65%) and 2x (red, ~17%) fibres (Figure 3A,B). There was also a small proportion of hybrid fibres. Overall, the proportion of fibre types in each muscle did not significantly differ between the four groups of mice (Figure 3B). Thus, AdipoRon did not induce a fibre switch towards a more oxidative phenotype in middle-aged obese mice, unlike in mdx mice.¹⁴ Fibre size, assessed by both cross-sectional area and minimum Feret's diameter, was also roughly similar in the different groups (not shown).

Next, by Bodipy staining, we quantified IMCL content and LD size on a fibre type and subcellular (peripheral vs. central) specific basis (Figures 3C and 4). The overall lipid content was higher in the peripheral (subsarcolemmal) region than at the

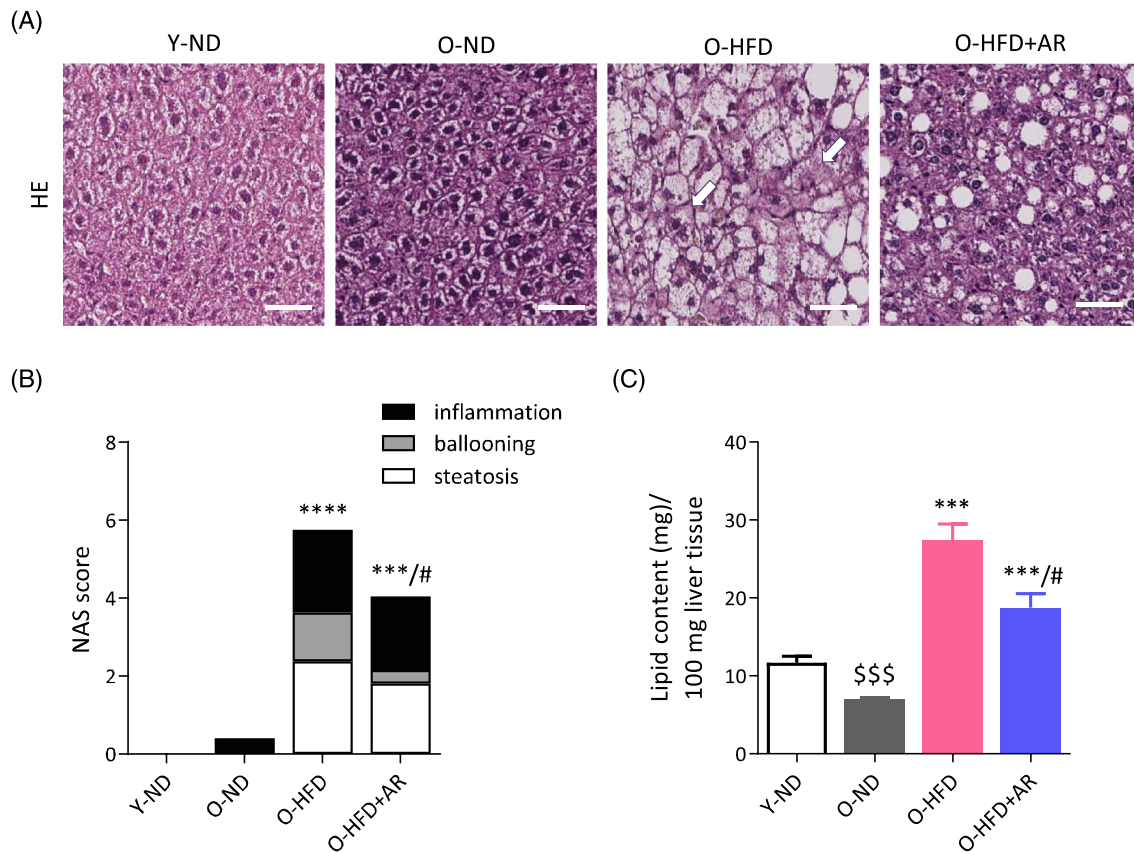


Figure 2 Chronic administration of AdipoRon reduces the severity of nonalcoholic fatty liver disease (NAFLD) in middle-aged obese mice. (A) Representative haematoxylin and eosin-stained liver sections from the different groups of mice. Arrows indicate hepatocellular ballooning, scale bar = 50 μ m. (B) Histological NAFLD activity score (NAS) calculated on sections like those shown in (A). (C) Lipid content in liver (biochemical measure). Data are means \pm SEM for 6 Y-ND, and 8–10 mice in the other three groups. Unless otherwise specified, statistical analysis was performed using one-way ANOVA followed by Tukey's test (comparing three groups of O-mice) or by unpaired two-tailed *t*-test (Y-ND vs. O-N). ^{SS}*P* < 0.001 versus Y-ND mice. ****P* < 0.001, *****P* < 0.0001 versus O-ND mice. #*P* < 0.05 versus O-HFD mice.

centre of the myofibre. Peripheral IMCL accumulation has been associated with insulin resistance^{18,19} and could also exert a mechanical stress on sarcolemma. As shown on *Figure 3C*, the plasma membrane presented scalloped edges (arrows) due to the presence of large subsarcolemmal LDs. In Types 1 and 2a fibres of soleus, IMCL content (expressed as the percentage of stained area) was significantly increased in O-ND mice compared with that in the Y-ND ones (both centrally and peripherally) and was not significantly modified by HFD (*Figure 4A*). However, when compared with HFD-fed mice, AdipoRon reduced total IMCL content in both fibre types. In EDL (type 2x and type 2b fibres), IMCL content of O-ND mice was roughly similar to that of Y-ND mice (except for the periphery in 2x fibres) (*Figure 4B*). By contrast, this content was significantly increased by HFD in both fibre types (compare O-HFD vs. O-ND mice). AdipoRon drastically reduced HFD-induced IMCL accumulation in both types of fibres and in both regions. Moreover, it tended to reduce LD size in soleus (especially in 2a fibres) and in EDL in both fi-

bre types, both centrally and peripherally (*Figure 4C,D*). Taken together, these results indicate that AdipoRon strikingly reversed IMCL accumulation either due to ageing in oxidative fibres or to HFD in glycolytic ones. It reduced LD size as well.

We then analysed whether AdipoRon enhanced fatty acid oxidation by stimulating the AMP-activated protein kinase (AMPK)-peroxisome proliferator-activated receptor γ coactivator-1 α (PGC-1 α /*Ppargc.1a*) axis (*Figure S2*).⁶ The phosphorylated and active form of AMPK (P-AMPK) and protein levels of PGC-1 α doubled under AdipoRon when compared with the other two groups of O-mice. The expression of relevant target genes of this transcriptional co-activator was (or tended to be) increased by AdipoRon, including those involved in fatty acid oxidation or energy dissipation (represented by dark blue boxes, part 1 on *Figure S2*). Thus, AdipoRon enhanced (or tended to enhance) mRNA abundance of medium-chain acyl-CoA dehydrogenase (*Acdm*), acyl-CoA oxidase (*Acox*) and uncoupling protein 3 (*Ucp3*) (*Figure 5B*).

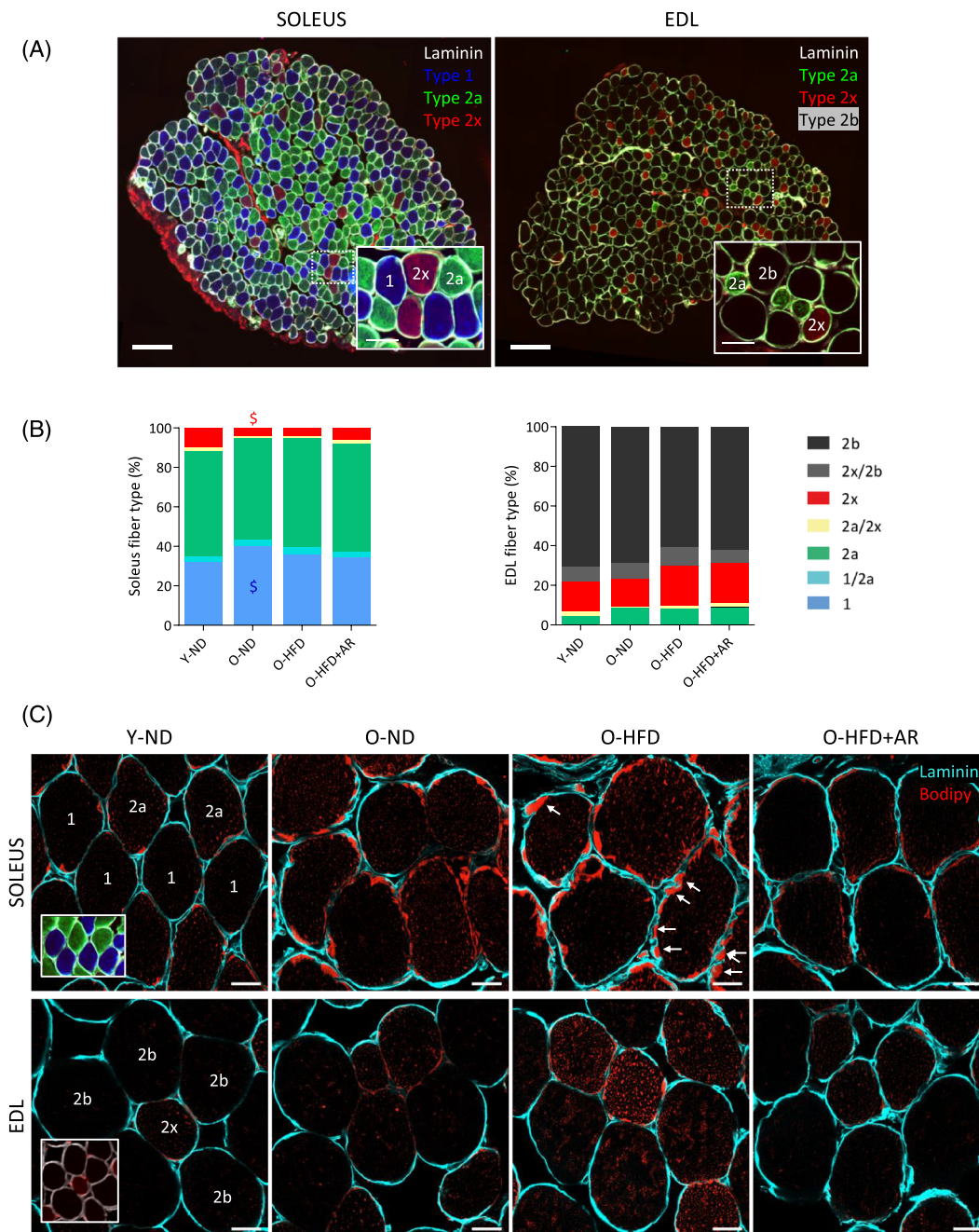


Figure 3 Effects of AdipoRon on fibre type composition and lipid infiltration in soleus and EDL from middle-aged obese mice. Fibre typing and Bodipy staining were performed on serial muscle cross-sections in an oxidative (soleus) and a glycolytic (EDL) muscle. (A) Fibre typing was carried out by immunofluorescence staining of different myosin heavy chains isoforms (MyHCs). Type 1 fibres were labelled in blue, type 2a in green, 2x in red while 2b were nonlabelled (black). Laminin antibody was used to delineate basal membrane (white). Representative sections for each group are shown. Scale bar = 200 μ m. *Insets*: Higher magnification of immunostaining images (scale bar = 50 μ m). (B) Fibre type proportion for each muscle in the 4 groups of mice. Data are means for six mice per group. Statistical analysis was performed using one-way ANOVA followed by Tukey’s test (comparing three groups of O-mice) or by unpaired two-tailed *t*-test (Y-ND vs. O-ND). ^S*P* < 0.05 versus Y-ND mice. (C) Bodipy staining of lipids (red) on muscle cross-sections to quantify IMCL content on a fibre type specific-basis. Laminin was coloured in cyan. Peripheral (subsarcolemmal, SS) lipid droplets (LDs) are usually more abundant than central ones. Arrows indicate scalloped edges of sarcolemma facing large SS LDs. Representative sections for six mice per group are shown. Scale bar = 20 μ m.

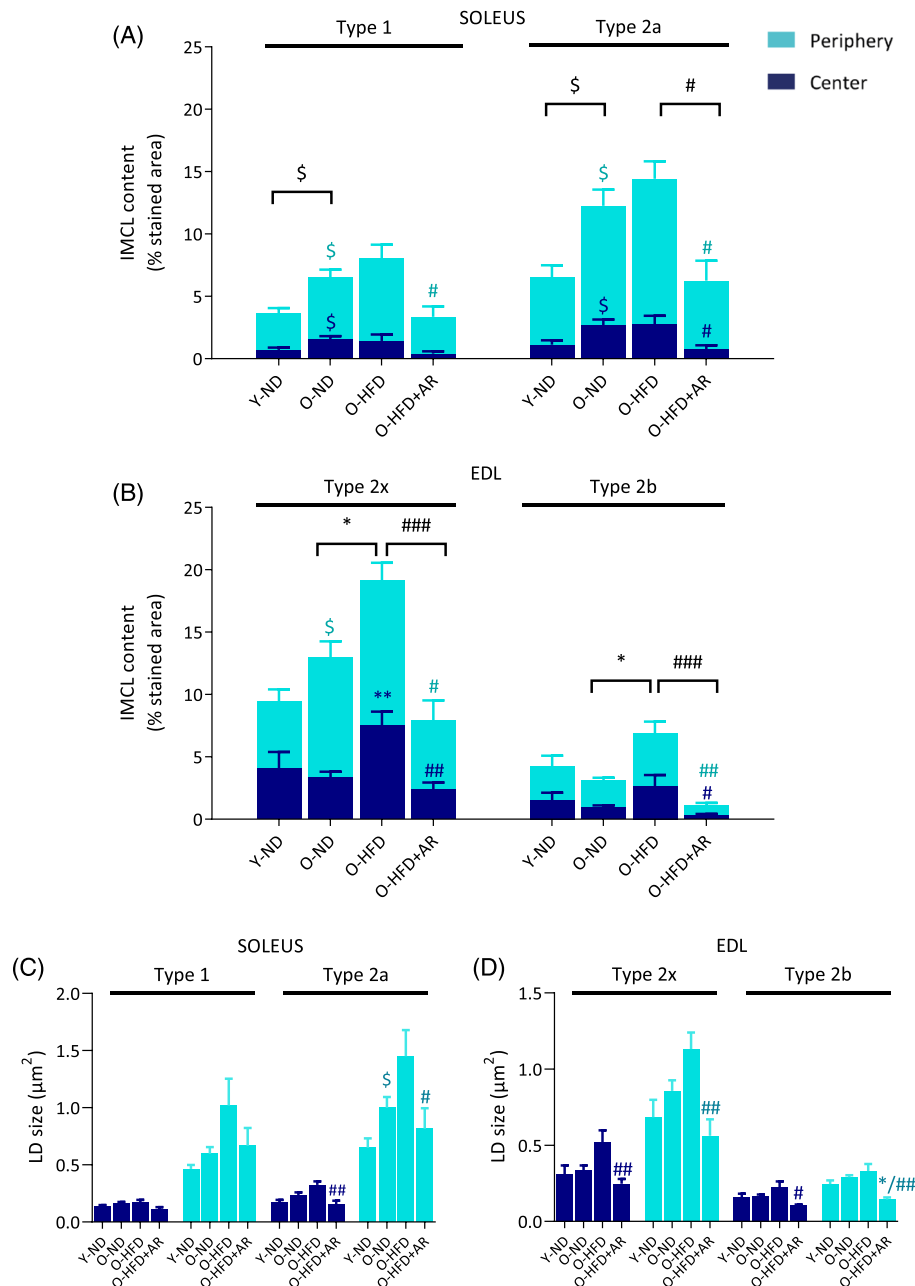


Figure 4 AdipoRon drastically blunts diet- or age-induced accumulation of intramyocellular lipids (IMCL) in middle-aged obese mice. (A) IMCL content of soleus in peripheral and central subcellular regions in type 1 and 2a fibres stained by Bodipy and (B) IMCL content of EDL in subcellular regions in type 2x and 2b fibres. IMCL content in each region was expressed as the percentage of stained area normalized to total fibre area. Symbols for differences among central regions are in dark blue, among peripheral regions in turquoise blue, and those for the total content in black. (C) LD size in peripheral and central subcellular regions in type 1 and 2a fibres from soleus and (D) in type 2x and 2b fibres from EDL. Data are means \pm SEM for five mice per group. Statistical analysis was performed using one-way ANOVA followed by Tukey's test (comparing three groups of O-mice) or by unpaired two-tailed *t*-test (Y-ND vs. O-ND). $^{\$}P < 0.05$ versus Y-ND mice. $^{*}P < 0.05$, $^{**}P < 0.01$ versus O-ND mice. $^{\#}P < 0.05$, $^{###}P < 0.01$, $^{####}P < 0.001$ versus O-HFD mice.

AdipoRon improves muscle mitochondrial function

PGC-1 α also promotes mitochondrial biogenesis and function via the transcriptional regulation of nuclear transcription fac-

tors such as nuclear respiratory factor-1 (NRF-1) (Part 2 on Figure S2). Expression of NRF-1 tended to be increased by AdipoRon (Figure 5C). Moreover, AdipoRon doubled the expression of mitochondrial transcription factor A (*Tfam*),

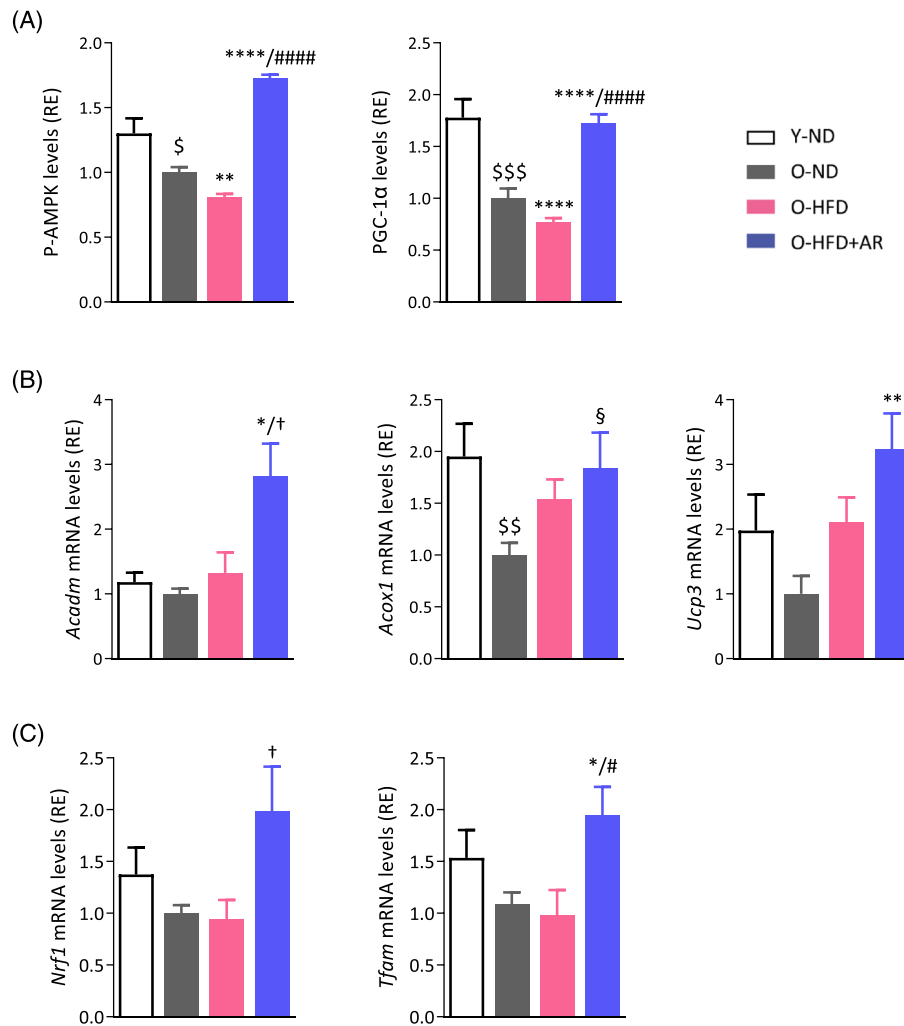


Figure 5 AdipoRon increases or tends to increase the expression of genes involved in fatty acid oxidation, mitochondrial biogenesis and function in soleus of middle-aged obese mice. (A) AMPK activity and protein levels of PGC-1 α (gastrocnemius), early signalling events of the cascade leading to enhancing effects on mitochondria. (B) mRNA levels of medium-chain acyl-CoA dehydrogenase (*Acadm*) and acyl-CoA oxidase 1 (*Acox1*) implicated in fatty acid oxidation and uncoupling protein 3 (*Ucp3*) in energy dissipation. (C) mRNA levels of nuclear respiratory factor-1 (*Nrf1*), a target gene of PGC-1 α and of mitochondrial transcription factor A (*Tfam*). mRNA levels were normalized to cyclophilin, and the subsequent ratios presented as relative expression compared with O-ND values. The active phosphorylated form of AMPK α (P-AMPK) and PGC-1 α protein levels were quantified by ELISA, and absorbance data were presented as relative expression compared with O-ND values. Data are means \pm SEM for 6 Y-ND, and 8–10 mice in the other three groups (A–C). Statistical analysis was performed by one-way ANOVA followed by Tukey's test (comparing three groups of O-mice) or by unpaired two-tailed *t*-test (Y-ND vs. O-ND). $^{\S}P < 0.05$, $^{\S\S}P < 0.01$, $^{\S\S\S}P < 0.001$ versus Y-ND mice. $^{\S}P = 0.059$, $^*P < 0.05$, $^{**}P < 0.01$, $^{****}P < 0.0001$ versus O-ND mice. $^{\dagger}P \leq 0.08$, $^{\#}P < 0.05$, $^{\#\#\#\#}P < 0.0001$ versus O-HFD mice.

downstream of NRF1, which binds to mitochondrial DNA (mtDNA) and activates mitochondrial biogenesis and function²⁰ (Figures 5C and S2).

Myofibre mitochondrial content was assessed by immunodetection of the translocase of outer mitochondrial membrane 20 (TOMM20) in soleus and EDL, in a fibre- and subcellular-specific way (Figures 6 and S2). As described,²¹ in soleus, type 2a fibres, which are more oxidative than type 1, have a higher mitochondrial content (Figure 6A,B; compare the percentage of stained area between the 2 fibre types). Likewise, in EDL, type 2x fibres have more mitochondria than 2b, which are more glycolytic and whose mitochondrial con-

tent was barely detectable²¹ (Figure 6A,B). Mitochondria were usually more abundant in the subsarcolemmal region. In soleus, total mitochondrial content rose under HFD (mainly due to an increase in subsarcolemmal mitochondria) in line with other reports,²² but this content was not influenced by the treatment. Mitochondria content decreased with age in 2x fibres (Figure 6B). Overall, there was no major change in mitochondrial content induced by AdipoRon in any muscle. Yet, as shown in Figures 6C and S3, (immuno)fluorescence co-labelling (TOMM20/Bodipy) revealed physical contacts between LDs and mitochondria, which may facilitate the trafficking of fatty acids released from LDs to mitochondria,

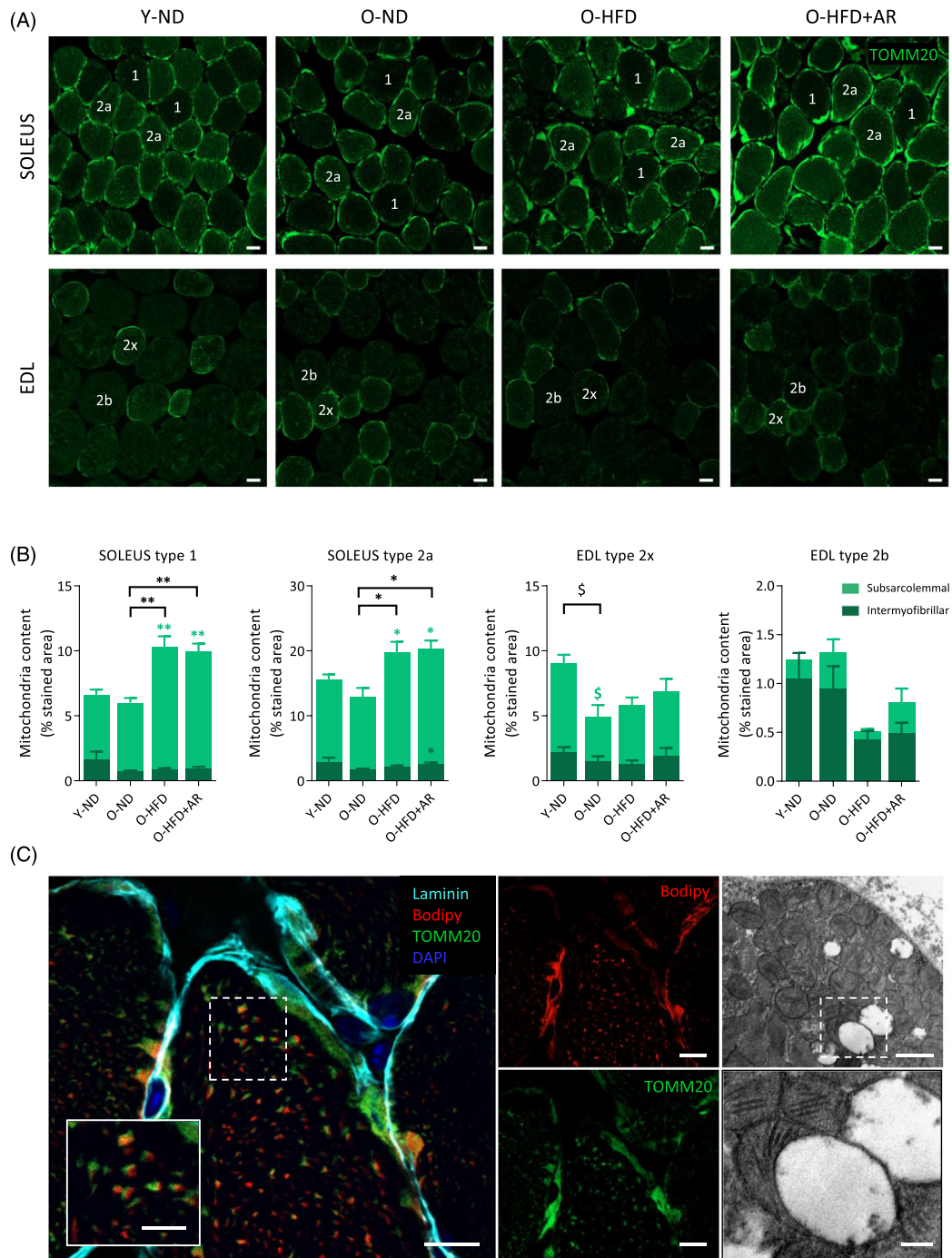


Figure 6 Quantification of mitochondrial content in muscle of middle-aged obese mice treated or not with AdipoRon. (A) Mitochondrial content was assessed by immunodetection of the translocase of outer mitochondrial membrane 20 (TOMM20) in soleus and EDL from the four groups of mice on a fibre dependent manner. Representative images for each group are shown. Scale bar = 20 μm . (B) Quantification of mitochondrial content in peripheral (subsarcolemmal) and central (intermyofibrillar) subcellular regions for each fibre type in soleus or EDL. Mitochondrial content in each region was expressed as the percentage of stained area normalized to total fibre area. Data are means \pm SEM for 5–6 mice per group. Statistical analysis was performed by one-way ANOVA (comparing three groups of O-mice) or by unpaired two-tailed *t*-test (Y-ND vs. O-ND). $^{\$}P < 0.05$ versus Y-ND mice. $*P < 0.05$, $**P < 0.01$ versus O-ND mice. Symbols for differences among central regions are in dark green, among peripheral regions in light green, and those for the total content in black. (C) Lipid droplet (LD)-mitochondrion contacts. *Left*, confocal fluorescence micrographs of soleus from an O-HFD mouse: LDs were stained with Bodipy in red, mitochondria with anti-TOMM20 in green, the edge of the fibre with anti-laminin in cyan and nuclei with DAPI in blue. Some mitochondria co-localized with LDs when channels were merged. Scale bar = 10 μm . Inset: Higher magnification (scale bar = 5 μm). *Right*, transmission electron micrograph of rectus femoris from an O-HFD + AR mouse illustrating LD-mitochondrion contact. Scale bar = 1 μm (*top right*) and 0.25 μm (*inset, bottom right*).

where they are oxidized. Transmission electron microscopy (TEM) confirmed such close contacts (Figure 6C).

Because mitochondrial content did not increase with AdipoRon, while the treatment significantly reduced LD accumulation, we tested the hypothesis that AdipoRon mainly enhanced mitochondrial function. We measured the activity of two respiratory enzymes: Cytochrome C oxidase (COX), whose catalytic subunits are partly encoded by mtDNA, and succinate dehydrogenase (SDH), which is entirely encoded by nuclear cDNA (Figure S2). For COX, the proportion of dark fibres indicating high activity was increased in O-HFD + AR compared with the other groups of old mice (+34% vs. O-ND and +26% vs. O-HFD) while the proportion of pale fibres was decreased (Figure 7A,B). In addition, COX activity was reduced in O-ND mice compared with Y-ND, reflecting impaired mitochondrial activity with ageing. By contrast, SDH activity was roughly similar between the different groups of mice (Figure 7C,D). As mtDNA integrity is essential for the successful synthesis of active COX, these results indicate that mitochondrial function, which is impaired with ageing, was improved and even corrected with AdipoRon.

Because abnormal mitochondrial ultrastructure is associated with impaired mitochondrial function, we qualitatively analysed mitochondrial morphology by TEM in each group of mice. Figure 7E illustrates mitochondria and LDs in the subsarcolemmal region of the rectus femoris. The two groups of untreated old mice showed a greater abundance of aberrant mitochondria (painted in pale green): swollen mitochondria, organelles with disrupted cristae, vacuoles-like structure formation and reduced electron density of the matrix, whereas AdipoRon treatment alleviated these abnormalities (normal mitochondria in dark green).

AdipoRon reduces aged-related tubular aggregate and cylindrical spiral formation

Tubular aggregates (TAGs) and cylindrical spirals (CSs) were observed in rectus femoris of middle-aged mice. These are two distinct ultrastructural abnormalities that share similar histochemical staining characteristics.²³ By bright field microscopy, they appear as pale or slightly basophilic inclusions with haematoxylin–eosin, bright red ones with Gomori trichrome (Figure 8A) or unstained with COX or SDH detection (see Figure 7A,C). By electron microscopy, TAGs may display different forms, the most typical being straight single-walled or double-walled tubules, regularly organized in tightly packed aggregates with a para-crystalline order, while CSs appear as accumulations of spiral lamellae (Figure 8B).

These abnormal structures (bright red inclusions) were quantified on Gomori sections from the four groups of mice (Figure 8C). They were almost absent in young mice but were much more abundant in old ones. Strikingly, AdipoRon reduced by almost 50% the accumulation of these

ageing-related structures in myofibres. Because these structures represent intracellular bins for dysfunctional accumulation of proteins, we instigated autophagy-related players (Figures 8D and S4). Autophagy marker light chain 3 (LC3) II/I ratio was unchanged in the four groups of mice. However, p62 expression was reduced by 53% in O-HFD + AR mice compared with O-ND, suggesting that AdipoRon stimulates autophagy. Moreover, AdipoRon enhanced the phosphorylation of UNC-51 like kinase (ULK1) at Ser555 (~40% vs. other O-mice), in line with the fact that AMPK phosphorylates and activates this autophagy marker.²⁴

AdipoRon and muscle inflammation

Lastly, we studied the potential anti-inflammatory effect of AdipoRon on the muscle. AdipoRon reduced approximately 20% of NF- κ B activity, assessed by the active and phosphorylated form of the p65-subunit (Figure S5). However, the other markers of inflammation (TNF α , IL1- β and CD68) or oxidative stress (peroxiredoxin 3 and hydroxy-2-nonenal), measured either at the mRNA or protein level, were extremely low or undetectable and were not influenced by AdipoRon (not shown).

Discussion

Long-term administration of AdipoRon improves exercise endurance, attenuates ectopic lipid deposit and reduces degenerative markers in the muscle of obese and middle-aged mice. Thus, AdipoRon administration close to 1 year promotes healthy ageing in mice on a normal genetic background. These findings extend the effects observed in mice with a genetic defect (db/db) where the marked alleviation of the severe diabetic status by AdipoRon was a major confounding factor.¹⁰ This is the longest treatment with AdipoRon ever reported so far. Its persisting effects indicate that there is no habituation to this compound. This long treatment was also well tolerated and safely promotes beneficial effects.

Plasma ApN levels were low in old mice compared with young ones (O-ND vs. Y-ND). Likewise, in a 'classical' population of geriatric patients, those who were also more likely to be functionally dependent had lower plasma ApN levels than the others.²⁵ Conversely, in most studies, plasma ApN levels were higher among centenarians than in elderly individuals, and those levels correlated with a preferable metabolic phenotype.²⁶ Hence, there could be a rationale for therapeutic correction of ApN in ageing.

By reducing ectopic lipids in both liver and muscle, AdipoRon protects obese and middle-aged mice against burdens associated with the metabolic syndrome: NASH and myosteatosis. NAFLD is the most common chronic liver

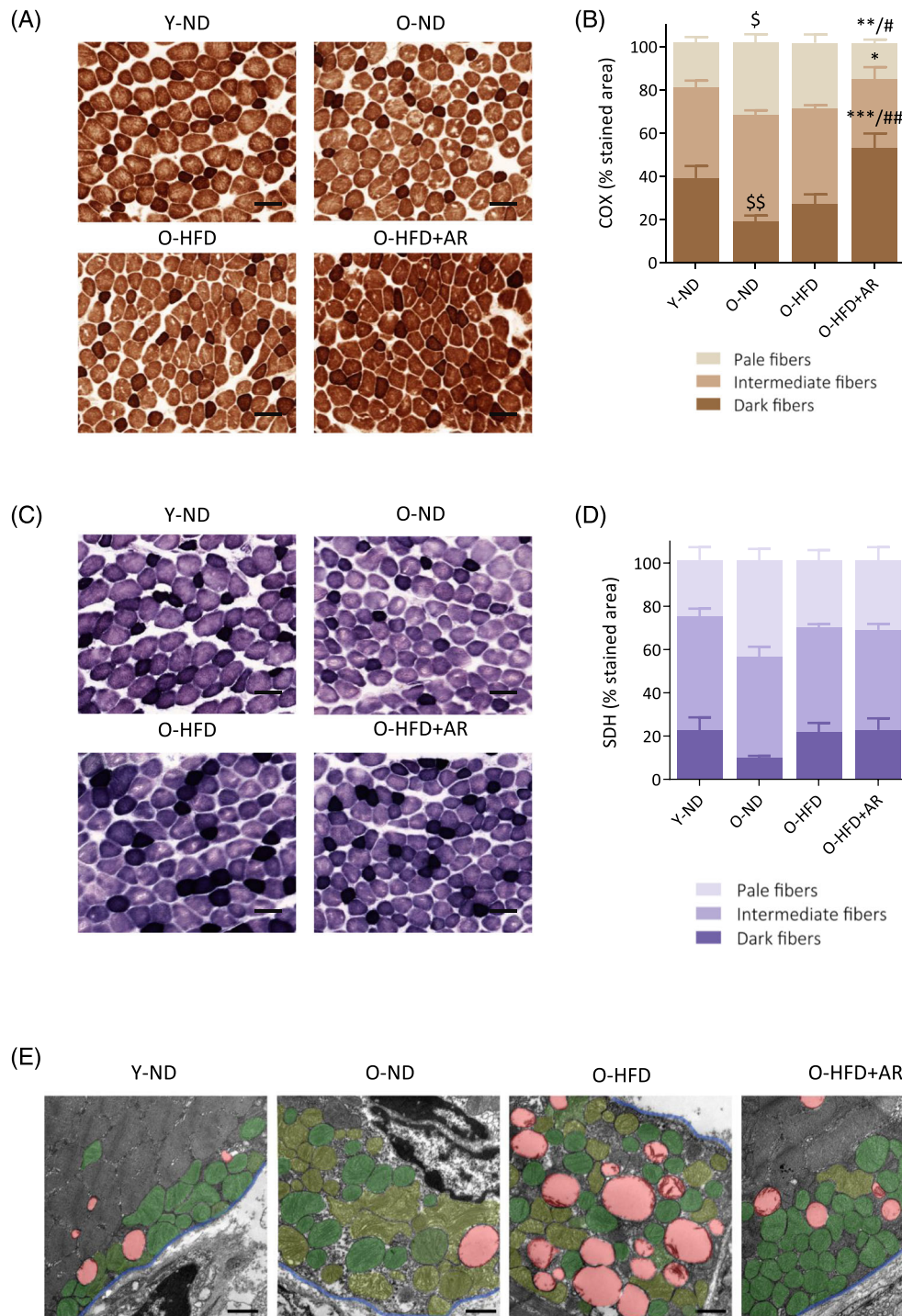


Figure 7 Chronic administration of AdipoRon enhances mitochondrial function and protection in muscle of middle-aged obese mice. (A,C) Histochemistry staining of COX and SDH activity in the rectus femoris of the four groups mice, the darkest colour being associated with the highest activity. Representative images of both stainings for each group are shown. Scale bar = 100 μ m. (B,D) quantification of COX and SDH activity. Activity was expressed as the percentage of stained area normalized to the cross-sectional area of the muscle, for each of the three staining intensities (set up as corresponding to pale, intermediate or dark colour). Data are means \pm SEM for 4–6 mice per group. Statistical analysis was performed by one-way ANOVA (comparing three groups of O-mice) or by unpaired two-tailed *t*-test (Y-ND vs. O-ND). $^{\$}P < 0.05$, $^{\$\$}P < 0.01$ versus Y-ND mice. $^*P < 0.05$, $^{**}P < 0.01$, $^{***}P < 0.001$ versus O-ND mice. $^{\#}P < 0.05$, $^{\#\#}P < 0.01$ versus O-HFD mice. (E) Transmission electron micrographs of mitochondria in the subsarcolemmal region of rectus femoris in the four groups of mice. For the sake of clarity, abnormal mitochondria are false-coloured in pale green, while normal mitochondria are coloured in dark green, LDs in red and the blue line delimits the sarcolemma. Representative images of each group are shown. Scale bar = 1 μ m.

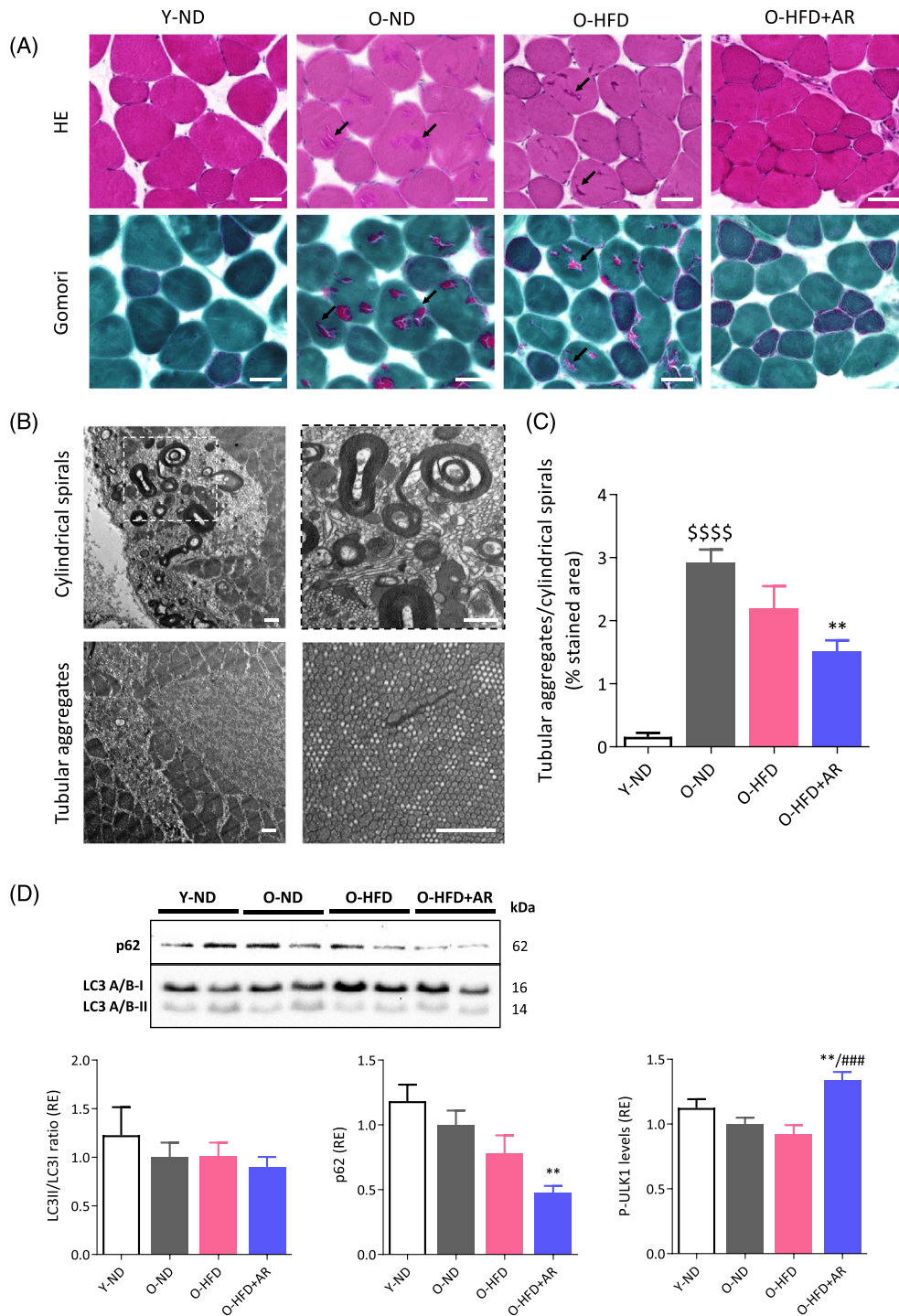


Figure 8 Chronic administration of AdipoRon reduces aged-related tubular aggregate (TAG) and cylindrical spiral (CS) formation in muscle of middle-aged obese mice. (A) TAGs and CSs (indicated by arrows) appear in rectus femoris from the different groups of mice as pale or slightly basophilic inclusions with haematoxylin–eosin (HE) and bright red ones with Gomori Trichrome. Scale bars = 50 μ m. (B) Confirmation of these structures by transmission electron microscopy. Scale bars = 1 μ m. (C) Quantification of TAG/CS abundance expressed as the percentage of stained area (bright red inclusions) normalized to the cross-sectional area of the muscle after Gomori trichrome. Data are means \pm SEM for six mice per group. (d) Effects of AdipoRon on autophagy markers in muscle from the four groups of mice. LC3II/LC3I ratio and p62 were analysed by western blotting and the phosphorylated form (Ser555) of ULK1 by ELISA. p62 levels were normalized to Ponceau S staining (shown in Figure S4). Results were then presented as relative expression compared to O-ND values. Data are means \pm SEM for 6–10 mice per group. Statistical analysis was performed by one-way ANOVA followed by Tukey's test (comparing three groups of O-mice) or by unpaired two-tailed t-test (Y-ND vs. O-ND). $^{5555}P < 0.0001$ versus Y-ND mice. $^{**}P < 0.01$ versus O-ND mice. $^{####}P < 0.001$ versus O-HFD mice.

disease in the world due to the rising prevalence of obesity and ageing. NAFLD encompasses steatosis and NASH. NASH is the severe form of NAFLD with lobular inflammation and hepatocyte ballooning; this stage has a clear potential of progression to cirrhosis and hepatocellular cancer.¹⁷ Herein, in spite of receiving HFD for more than 1 year, mice treated with AdipoRon exhibit NAFLD that does not progress into NASH, as assessed by the NAS score. These data extend the decreased hepatic lipid content measured by chemical extraction after 2 weeks of AdipoRon in HFD mice or db/db mice¹⁰ and the lessening of liver injury caused by toxic agents under AdipoRon.¹²

The protective effects of AdipoRon against myosteatosis have been poorly studied so far.¹⁰ Yet myosteatosis is emerging as a public health problem. It increases with age and obesity and is recognized to negatively correlate with muscle mass, strength and mobility, and disrupts metabolism (insulin resistance and diabetes).⁴ It is also a negative prognostic factor for cancer,²⁷ cardiovascular disease²⁸ or NAFLD.¹⁷ IMCLs are predominantly stored in LDs to serve as metabolic fuel during physical exercise. However, when lipid supply exceeds demand, or when mitochondria become dysfunctional, IMCLs are also implicated in muscle insulin resistance as in obesity and type 2 diabetes.^{29,30} Yet, endurance athletes have similar, if not higher, IMCL content than obese patients with type 2 diabetes, while maintaining high insulin sensitivity. This 'athlete's paradox' is explained by a more nuanced appraisal of muscle LDs, including localization and size.^{19,29} Peripheral LDs exert a more deleterious effect on insulin sensitivity than central ones, which are more dedicated to produce fuel for contraction.^{19,29} LD size also plays a role on overall metabolism as this parameter is inversely correlated to insulin sensitivity and physical fitness.^{18,29} In fact, smaller LDs exhibit a larger surface area for lipase action and thus potentially have a greater capacity to mobilize lipids.²⁹ By using Bodipy staining, we quantified IMCL content and analysed LD size and subcellular distribution in a fibre-specific manner. Our study highlights a differential impact of ageing and dietary fat overload on IMCL content according to fibre type. Thus, ageing promotes accumulation of IMCLs in oxidative fibres while dietary fat overload promotes such an accumulation in glycolytic ones. The latter observation is concordant with the elevated fatty acid content observed in EDL, but not in soleus, after 5 weeks of HFD administration to mice.³¹ The lower impact of HF overload on soleus may be explained by the concomitant upregulation of mitochondrial content in oxidative fibres²² (see *Figure 6B*), which may partly cope with lipid excess. A novel and important finding is that AdipoRon strikingly reversed IMCL accumulation whether due to ageing in oxidative fibres (Types 1 and 2a) or to HFD in glycolytic ones (Types 2x and 2b). This correction occurs in both subcellular regions. The size of LDs, especially subsarcolemmal ones was reduced as well.

Besides being associated with adverse metabolic outcomes, large LDs could also affect muscle contractile capacity as previously suggested.³² Herein, we proposed that large subsarcolemmal LDs could exert a mechanical stress on plasma membrane as supported by scalloped edges of sarcolemma. Other mechanisms could also contribute to impair contractility: inhibition of sarco/endoplasmic reticulum Ca^{2+} -ATPase (SERCA) or of mitochondrial function by fatty acid metabolites for instance.³¹ Even in single myofibre isolated from obese older or normal weight subjects, there was an inverse relationship between IMCL content and fibre contraction, power and force development, raising the possibility of a vicious circle between IMCL accumulation and functional muscle impairment, thereby further worsening obesity.³³ Taken together, our data show that AdipoRon potentially protects against myosteatosis caused by ageing or calorie excess. As total numbers of fibres in each muscle and cross-sectional area for each fibre type were similar between the four groups of mice, this raises the possibility that the true contractile mass was actually higher in AdipoRon mice due to lower IMCL accumulation. When comparing the protection afforded by AdipoRon against ectopic lipid deposit in the liver and the skeletal muscle, the alleviation of steatosis was more drastic in the muscle where the correction was complete.

We next examined the mechanisms underlying the marked reduction of myosteatosis and focused on mitochondrial biogenesis and function, which are known to be stimulated by AdipoRon.¹⁰ The mitochondrial content, assessed by TOMM20 staining was not modified by AdipoRon, while COX activity was enhanced. As mtDNA integrity is essential for synthesis of active COX, these results suggest that mitochondrial function is impaired with ageing,³⁴ but then markedly improved with AdipoRon. Consistently, the expression of genes involved in fatty acid oxidation or energy dissipation was—or tended to be—increased as well, in line with a previous report.¹⁰ The beneficial effects of AdipoRon on mitochondria are reinforced by TEM analysis indicating that there were less damaged—presumably less dysfunctional—mitochondria in the muscle of AR-treated mice than in age-matched untreated groups. Comparing these results with those of TOMM20, we assume that some damaged mitochondria could still remain immunoreactive for TOMM20. Taken together, these data indicate that AdipoRon protects against the decline of mitochondrial function due to ageing.

By using TEM, we fortuitously found the presence of tubular aggregates (TAGs) and cylindrical spirals (CSs) in glycolytic myofibres of middle-aged mice.^{35,36} These structures correspond to abnormal accumulation of sarcoplasmic reticulum (SR) components. Immunohistochemical studies showed that TAGs were derived from the whole SR, while CSs were derived merely from the longitudinal one.^{23,35} In humans, the presence of TAGs defines a clinically heterogeneous group of disorders termed TA myopathies (TAM) characterized by muscle

weakness, while CSs have been implicated in some rare familial muscle disorders.^{23,35} Yet, the presence of TAGs or CSs has not been studied in the elderly, but TAGs virtually identical to those of TAM patients have been found in ageing mice.³⁶ TAG abundance in old mice is accompanied by impaired ability to restore internal Ca^{2+} stores from extracellular space, which could contribute to muscle weakness. Herein, an original finding is that AdipoRon strikingly reduced the accumulation of TAGs and CSs in middle-aged mice and improved exercise endurance. In line with this observation, long-term regular exercise counteracted TAG formation in aged mice, while improving the capability of fibres to use extracellular Ca^{2+} .³⁶

Because AdipoRon reduced damaged mitochondria as well as TAGs and CSs, we speculated that this mimic could stimulate autophagy in the muscle of middle-aged obese mice. Different lines of evidence indicate that autophagy declines with ageing, while autophagy stimulation may have beneficial effects on lifespan.³⁷ We found no changes in autophagy markers in our two groups of middle-aged mice that did not receive AdipoRon. However, such changes are usually observed in older mice (~24 months).³⁸ Yet, AdipoRon activated the phosphorylation (Ser555) of ULK1, an autophagy marker under the control of AMPK.²⁴ It also markedly decreased the p62 protein, a receptor for cargo including protein aggregates destined for clearance.³⁷ Taken together, these data suggest that autophagy clearance was actually stimulated by AdipoRon in the muscle, in line with other studies.^{39,40}

AdipoRon is known to increase exercise endurance.¹⁰ Here, we extend these data to severely obese and middle-aged mice. Improved endurance was linked to preserved mitochondrial function, higher lipid oxidation and alleviation of myosteatosis. Reduced accumulation of dysfunctional SR proteins and improved capability of fibres to use extracellular Ca^{2+} could contribute as well. Conversely, prevention of muscle dysfunction in aged mice thanks to endurance training was attenuated by neutralizing antibodies against ApN or AdipoR1.⁴¹ The better performance of AR mice was not due to a higher motivation of these mice: A panel of behavioural tests did not demonstrate any attitude differences between our HFD mice treated or not (not shown), unlike data obtained in a mouse model of depression.

In conclusion, long-term AdipoRon treatment enhances muscle endurance in obese middle-aged mice and protects

the skeletal muscle and the liver from the adverse metabolic and degenerative effects of ageing and calorie excess. By promoting 'healthy ageing', AdipoRon could hence serve as a crucial step towards enhancing both healthspan and lifespan.

Acknowledgements

This work was supported by grants from UCL University (Research project FSR 2017), *Société Francophone du Diabète/Roche Diabetes Care 2020* and Fund for Scientific Research—FNRS (Research Credit 35275437, 2019). M. A. -S. is *Chargé de Recherches* and C. M. S. has received a fellowship from the FRIA. M. A. D. -L. d. C. received a fellowship from the Wallonie-Bruxelles International Excellence Program.

We are grateful to Caroline Bouzin and the IREC imaging platform for the use of the equipment and their aid, to Professor Philippe Gailly and Dr. Olivier Schakman for providing the necessary equipment and the know-how for the in vivo functional tests. We thank Camille Pichon for her involvement in the analysis of micro-CT scans; Marie-Christine Many and Peter Van den Bergh for their help in the interpretation of TEM images; Véronique Van Den Berge and Corinne Picalausa for their technical support; Laura De Cock, Alice Monnier and Marie Clerbois for their participation in mice experiments and tissue analysis. We also thank Greetje Vande Velde (MoSAIC, KU Leuven) for providing the micro-CT scan and the personnel of the microscopy services (CITIUS, *Universidad de Sevilla*) for their technical support for transmission electron microscopy.

All authors certify that they comply with the ethical guidelines for authorship and publishing in the *Journal of Cachexia, Sarcopenia and Muscle*.⁴²

Conflict of interest

Authors declare that no conflict of interest exists.

Online supplementary material

Additional supporting information may be found online in the Supporting Information section at the end of the article.

REFERENCES

1. Tieland M, Trouwborst I, Clark BC. Skeletal muscle performance and ageing. *J Cachexia Sarcopenia Muscle* 2018;**9**:3–19.
2. Fakhouri TH. Prevalence of obesity among older adults in the United States, 2007–2010. *NCHS Data Brief* 2012;**106**: 1–8.
3. Tam BT, Morais JA, Santosa S. Obesity and ageing: two sides of the same coin. *Obes Rev* 2020;**21**:e12991.
4. Correa-de-Araujo R, Addison O, Miljkovic I, Goodpaster BH, Bergman BC, Clark RV, et al. Myosteatosis in the context of skeletal muscle function deficit: an Interdisciplinary Workshop at the National Institute on Aging. *Front Physiol* 2020;**11**:963.
5. Alqahtani SA, Schattenberg JM. NAFLD in the elderly. *Clin Interv Aging* 2021;**16**: 1633–1649.
6. Abou-Samra M, Selvais CM, Dubuisson N, Brichard SM. Adiponectin and its mimics

- on skeletal muscle: insulin sensitizers, fat burners, exercise mimickers, muscling pills... or everything together? *Int J Mol Sci* 2020;**21**:2620.
7. Abou-Samra M, Lecompte S, Schakman O, Noel L, Many MC, Gailly P, et al. Involvement of adiponectin in the pathogenesis of dystrophinopathy. *Skelet Muscle* 2015; **5**:25.
 8. Otabe S, Yuan X, Fukutani T, Wada N, Hashinaga T, Nakayama H, et al. Overexpression of human adiponectin in transgenic mice results in suppression of fat accumulation and prevention of premature death by high-calorie diet. *Am J Physiol Endocrinol Metab* 2007;**293**:E210–E218.
 9. Li N, Zhao S, Zhang Z, Zhu Y, Gliniak CM, Vishvanath L, et al. Adiponectin preserves metabolic fitness during aging. *Elife* 2021; **10**:10.
 10. Okada-Iwabu M, Yamauchi T, Iwabu M, Honma T, Hamagami KI, Matsuda K, et al. A small-molecule AdipoR agonist for type 2 diabetes and short life in obesity. *Nature* 2013;**503**:493–499.
 11. Zhang Y, Zhao J, Li R, Lau WB, Yuan YX, Liang B, et al. AdipoRon, the first orally active adiponectin receptor activator, attenuates postischemic myocardial apoptosis through both AMPK-mediated and AMPK-independent signalings. *Am J Physiol Endocrinol Metab* 2015;**309**:E275–E282.
 12. Wang Y, Wan Y, Ye G, Wang P, Xue X, Wu G, et al. Hepatoprotective effects of AdipoRon against d-galactosamine-induced liver injury in mice. *Eur J Pharm Sci* 2016;**93**: 123–131.
 13. Iwabu M, Okada-Iwabu M, Tanabe H, Ohuchi N, Miyata K, Kobori T, et al. AdipoR agonist increases insulin sensitivity and exercise endurance in AdipoR-humanized mice. *Commun Biol* 2021;**4**:45.
 14. Abou-Samra M, Selvais CM, Boursereau R, Lecompte S, Noel L, Bricard SM. AdipoRon, a new therapeutic prospect for Duchenne muscular dystrophy. *J Cachexia Sarcopenia Muscle* 2020;**11**:518–533.
 15. Balasubramanian P, Schaar AE, Gustafson GE, Smith AB, Howell PR, Greenman A, et al. Adiponectin receptor agonist AdipoRon improves skeletal muscle function in aged mice. *Elife* 2022;**11**:11.
 16. Jortay J, Senou M, Abou-Samra M, Noel L, Robert A, Many MC, et al. Adiponectin and skeletal muscle: pathophysiological implications in metabolic stress. *Am J Pathol* 2012;**181**:245–256.
 17. Nachit M, de Rudder M, Thissen JP, Schakman O, Bouzin C, Horsmans Y, et al. Myosteatosis rather than sarcopenia associates with non-alcoholic steatohepatitis in non-alcoholic fatty liver disease preclinical models. *J Cachexia Sarcopenia Muscle* 2021;**12**:144–158.
 18. Nielsen J, Christensen AE, Nellemann B, Christensen B. Lipid droplet size and location in human skeletal muscle fibers are associated with insulin sensitivity. *Am J Physiol Endocrinol Metab* 2017;**313**:E721–e730.
 19. Bergman BC, Goodpaster BH. Exercise and muscle lipid content, composition, and localization: influence on muscle insulin sensitivity. *Diabetes* 2020;**69**:848–858.
 20. Picca A, Lezza A, Leeuwenburgh C, Pesce V, Calvani R, Landi F, et al. Fueling inflamm-aging through mitochondrial dysfunction: mechanisms and molecular targets. *Int J Mol Sci* 2017;**18**:933.
 21. Schiaffino S, Reggiani C. Fiber types in mammalian skeletal muscles. *Physiol Rev* 2011;**91**:1447–1531.
 22. Hancock CR, Han DH, Chen M, Terada S, Yasuda T, Wright DC, et al. High-fat diets cause insulin resistance despite an increase in muscle mitochondria. *Proc Natl Acad Sci U S A* 2008;**105**:7815–7820.
 23. Brady S, Healy EG, Gang Q, Parton M, Quinlivan R, Jacob S, et al. Tubular aggregates and cylindrical spirals have distinct immunohistochemical signatures. *Journal of Neuropathology & Experimental Neurology* 2016;**75**:1171–1178.
 24. Bujak AL, Crane JD, Lally JS, Ford RJ, Kang SJ, Rebalka IA, et al. AMPK activation of muscle autophagy prevents fasting-induced hypoglycemia and myopathy during aging. *Cell Metab* 2015;**21**:883–890.
 25. Can B, Kara O, Kizirlarlanoglu MC, Arik G, Aycicek GS, Sumer F, et al. Serum markers of inflammation and oxidative stress in sarcopenia. *Aging Clin Exp Res* 2017;**29**: 745–752.
 26. Arai Y, Kamide K, Hirose N. Adipokines and aging: findings from centenarians and the very old. *Front Endocrinol (Lausanne)* 2019;**10**:142.
 27. Aleixo GFP, Shachar SS, Nyrop KA, Muss HB, Malpica L, Williams GR. Myosteatosis and prognosis in cancer: systematic review and meta-analysis. *Crit Rev Oncol Hematol* 2020;**145**:102839.
 28. Miljkovic I, Kuipers AL, Cauley JA, Prasad T, Lee CG, Ensrud KE, et al. Greater skeletal muscle fat infiltration is associated with higher all-cause and cardiovascular mortality in older men. *J Gerontol A Biol Sci Med Sci* 2015;**70**:1133–1140.
 29. Seibert JT, Najt CP, Heden TD, Mashek DG, Chow LS. Muscle lipid droplets: cellular signaling to exercise physiology and beyond. *Trends Endocrinol Metab* 2020;**31**: 928–938.
 30. Gemmink A, Schrauwen P, Hesselink MKC. Exercising your fat (metabolism) into shape: a muscle-centred view. *Diabetologia* 2020;**63**:1453–1463.
 31. Ciapaitė J, van den Berg SA, Houten SM, Nicolay K, Willems van Dijk K, Jeneson JA. Fiber-type-specific sensitivities and phenotypic adaptations to dietary fat overload differentially impact fast- versus slow-twitch muscle contractile function in C57BL/6J mice. *J Nutr Biochem* 2015;**26**: 155–164.
 32. Andruch DE, Ou Y, Melbouci L, Leduc-Gaudet JP, Auclair N, Mercier J, et al. Altered lipid metabolism impairs skeletal muscle force in young rats submitted to a short-term high-fat diet. *Front Physiol* 2018;**9**:1327.
 33. Choi SJ, Files DC, Zhang T, Wang ZM, Messi ML, Gregory H, et al. Intramyocellular lipid and impaired myofiber contraction in normal weight and obese older adults. *J Gerontol A Biol Sci Med Sci* 2016;**71**: 557–564.
 34. Chistiakov DA, Sobenin IA, Revin VV, Orekhov AN. Mitochondrial aging and age-related dysfunction of mitochondria. *Biomed Res Int* 2014;**2014**:238463.
 35. Xu JW, Liu FC, Li W, Zhao YY, Zhao DD, Luo YB, et al. Cylindrical spirals in skeletal muscles originate from the longitudinal sarcolemmal reticulum. *J Neuropathol Exp Neurol* 2016;**75**:148–155.
 36. Boncompagni S, Pecorai C, Michelucci A, Pietrangeli L, Protasi F. Long-term exercise reduces formation of tubular aggregates and promotes maintenance of Ca(2+) entry units in aged muscle. *Front Physiol* 2020; **11**:601057.
 37. Hansen M, Rubinsztein DC, Walker DW. Autophagy as a promoter of longevity: insights from model organisms. *Nat Rev Mol Cell Biol* 2018;**19**:579–593.
 38. Huang DD, Yan XL, Fan SD, Chen XY, Yan JY, Dong QT, et al. Nrf2 deficiency promotes the increasing trend of autophagy during aging in skeletal muscle: a potential mechanism for the development of sarcopenia. *Aging (Albany NY)* 2020;**12**: 5977–5991.
 39. Liu Y, Palanivel R, Rai E, Park M, Gabor TV, Scheid MP, et al. Adiponectin stimulates autophagy and reduces oxidative stress to enhance insulin sensitivity during high-fat diet feeding in mice. *Diabetes* 2015;**64**: 36–48.
 40. Ahlstrom P, Rai E, Chakma S, Cho HH, Rengasamy P, Sweeney G. Adiponectin improves insulin sensitivity via activation of autophagic flux. *J Mol Endocrinol* 2017;**59**: 339–350.
 41. Inoue A, Cheng XW, Huang Z, Hu L, Kikuchi R, Jiang H, et al. Exercise restores muscle stem cell mobilization, regenerative capacity and muscle metabolic alterations via adiponectin/AdipoR1 activation in SAMP10 mice. *J Cachexia Sarcopenia Muscle* 2017; **8**:370–385.
 42. von Haehling S, Morley JE, Coats AJS, Anker SD. Ethical guidelines for publishing in the Journal of Cachexia, Sarcopenia and Muscle: update 2021. *J Cachexia Sarcopenia Muscle* 2021;**12**:2259–2261.